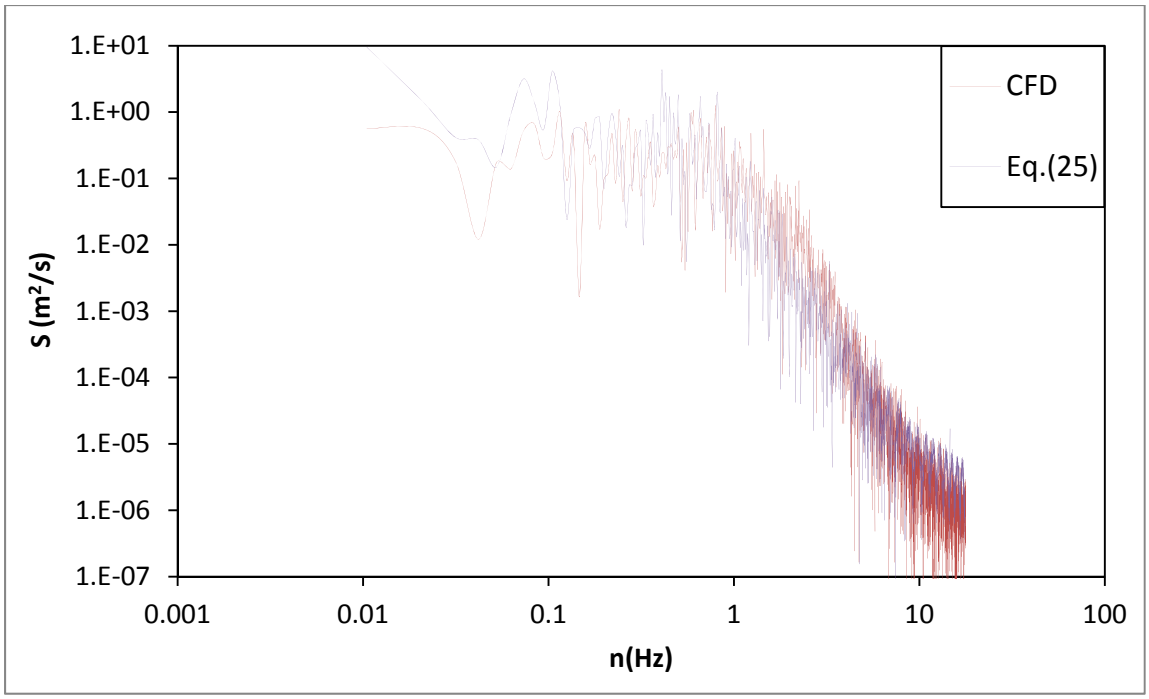

(b)

Figure 5 Spectra of the fluctuating ventilation rate (a) when the wind was parallel to the opening and (b) when the wind was normal to the opening

When the frequency is around 1, the corresponding eddy scale can penetrate into the opening. The results in Figure 5(a) indicate that, when the frequency is greater than 1, the red line will become much larger than the purple line. The difference is the energy of the penetrated eddies. When eddy penetration is considered, the blue line is closer to the red line (actual value). However, some discrepancies still exist because of the use of the Taylor Frozen hypothesis. This hypothesis is applied to convert the spectrum in the temporal domain into the spatial domain to filter the eddies based on their scales. It will lead to two problems: 1) the hypothesis assumes the flow is a homogeneous turbulent flow, which in this case may not be satisfied; 2) the mean velocity at the opening in Eqs. (19) and (27) was replaced by the mean wind velocity at the far field. Despite the two problems, this investigation used the Taylor Frozen hypothesis due to its simplicity and good overall accuracy.

Figure 5(b) shows the ventilation rate spectra when the wind is normal to the opening. The red line is the spectrum of the fluctuating ventilation rate calculated by CFD. The purple line is the spectrum of the ventilation rate calculated by Eq. (26) without considering the eddy penetration and agrees well with the CFD result. Compared with Figure 5(a), there was no eddy penetration when the wind was normal to the opening, which was consistent with the assumption made in Eq. (18).

4.4 Discussion

The model can predict the mean velocity component that is normal to the opening via

$$\overline{U_{\perp}}(z)=\begin{cases}\dfrac{C_d\sqrt{\left|C_p(z^{2/7}-z_0^{2/7})\right|}}{z_{ref}^{\ 1/7}}\overline{U}_{ref} & when\ C_p\cdot(z^{2/7}-z_0^{2/7})>0\\ -\dfrac{C_d\sqrt{\left|C_p(z^{2/7}-z_0^{2/7})\right|}}{z_{ref}^{\ 1/7}}\overline{U}_{ref} & when\ C_p\cdot(z^{2/7}-z_0^{2/7})\le 0\end{cases} \tag{28}$$

When $C_p\cdot(z^{2/7}-z_0^{2/7})>0$, the flow goes inwards to the building and when $C_p\cdot(z^{2/7}-z_0^{2/7})\le 0$, the flow goes outwards. As indicated by Eq.(28), when the pressure coefficient, C_p, is positive, the inflow will be in the upper part of the opening, and when it is negative, the inflow will be in the lower part of the opening.

This model assumes that the velocity along the opening width is the same. However, the results from CFD for Case 4 as shown in Figure 6(a) show that the velocity along the opening width is not uniform. Eq. (29) can be used to average the CFD results along the opening width to compare with those calculated by the empirical model:

$$\overline{U_{1\,ave}}(z)=\frac{\sum_k\left(\dfrac{\sum_i\overline{U}_{\perp}(t_i,x_k,z)}{\Delta t}\right)\Delta x_k}{l} \tag{29}$$

where k is the summation index through the opening width and Δt is the time period for the calculation. Then one can compare the velocity profile at the opening calculated by CFD with the profile by the empirical model.

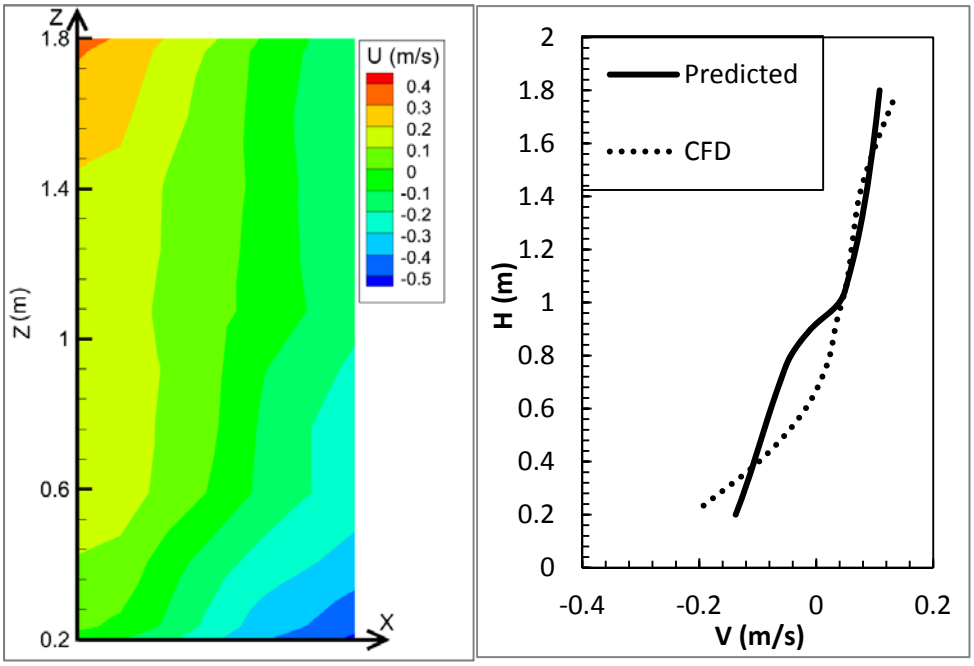

(a) (b)

Figure 6 (a) Y-velocity (normal to the opening) contour and (b) predicted Y-velocity profile versus averaged Y-velocity profile from CFD

Figure 6(b) compares the averaged velocity profile by CFD with that by the empirical model. In general, the two profiles are similar but with some differences in the lower part of the opening where the flow goes outwards. One possible reason is that the outflow will interact with the incoming wind and thus distort the flow field, which can be accounted for by CFD but not by the empirical model.

As mentioned in section 4.2, the wind direction will have a large influence on the ventilation rate. A more detailed analysis on the impact of wind direction on eddy penetration rate is necessary. Figure 7(a) shows the pressure coefficient for different wind directions. The pressure coefficient is normalized by the pressure coefficient when the incident angle is 90^o (the pressure coefficient for this case is negative). We selected 90^o because the eddy penetration rate is the largest. When the incident angle is smaller than 70^o, the normalized pressure coefficient is negative and the absolute value decreases as the incident angle increases. For an incident angle between 70º to 90º, the normalized pressure coefficient is positive and the absolute value increases as the incident angle increases. Note that the actual pressure coefficient will decrease monotonically with an increasing incident angle for windward cases because the wind load on the opening side reduces with the incident angle. For an incident angle larger than 90º, the pressure coefficient is around a certain value. This is mainly due to the weak zone at the leeward side [23,24].

Figure 7(b) depicts how the wind incident angle affects the eddy penetration. The eddy penetration rate is normalized by the penetration rate when the incident angle equals 90^o. According to Eq.(18), the two major factors that determine the eddy penetration rate are the

pressure coefficient and the parallel velocity component. The eddy penetration rate will increase with the absolute pressure coefficient and the parallel velocity. When the incident angle is smaller than 90^o, the parallel velocity will increase monotonically and yet the absolute pressure coefficient will first decrease and then increase. This will result in a dip of the eddy penetration rate at around 70^o where the pressure coefficient is close to zero. It should be noted that zero pressure coefficient may not exist in reality due to the fluctuation of the wind.

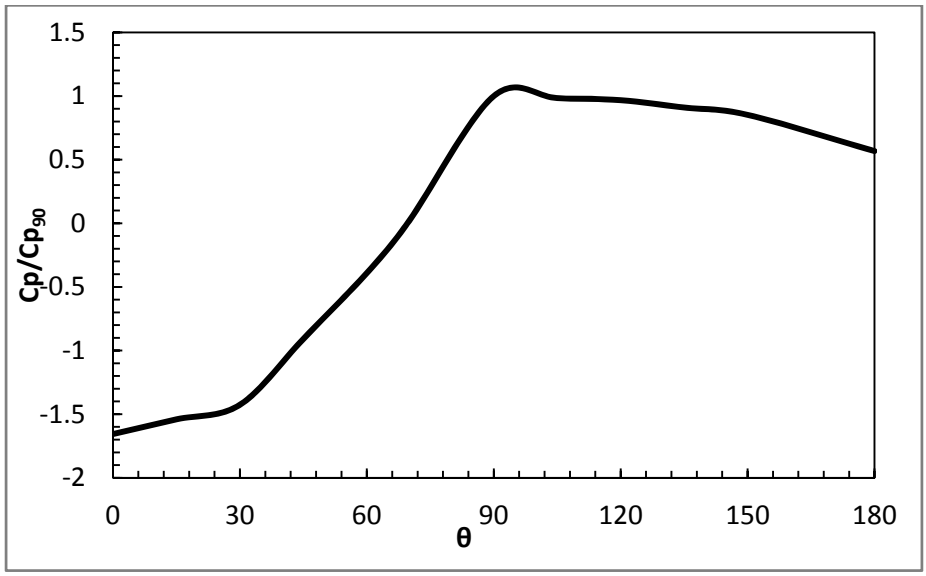

(a)

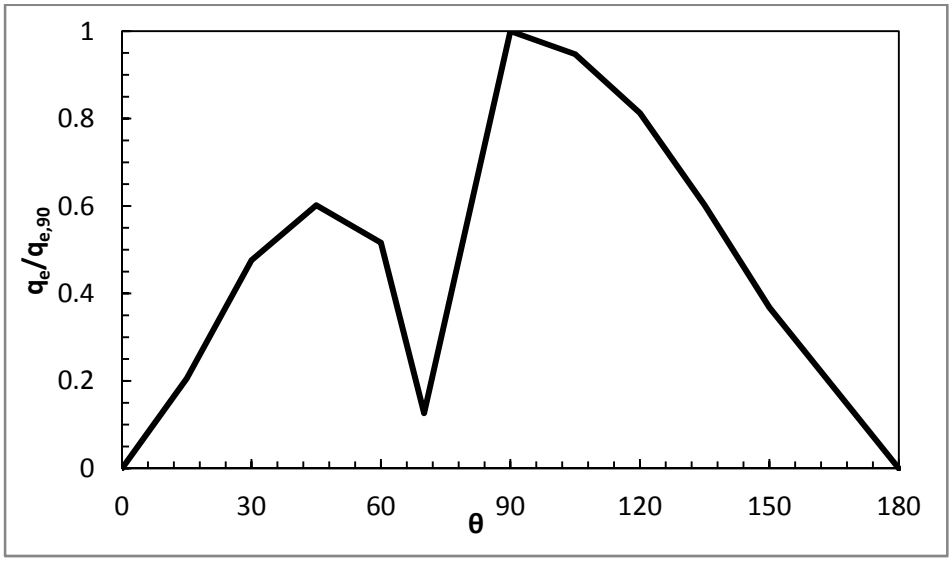

(b)

Figure 7 (a) Normalized pressure coefficient for different wind directions and (b) normalized eddy penetration rate for different wind directions

Other important factors influencing ventilation rate are the opening size and the elevation. The existing models for predicting ventilation rates often assume a linear relation between ventilation rate and opening size. Our model (Eqs. (15), (16), and (19)) shows that the opening height and width will result in non-linearity of the ventilation rate for single-sided ventilation. The effective velocity at the opening is defined as

$$U_{eff} = \frac{Q}{\frac{A}{2}} \tag{30}$$

where Q can be either mean ventilation rate or eddy penetration rate. Figure 8**Error! Reference source not found.** shows the influence of opening size on the effective velocity. The effective velocity is normalized by that of unit opening width or unit height. The solid line represents the effective eddy penetration velocity. As the opening width increases, the effective eddy penetration velocity also increases because more eddies can penetrate into the opening. Since the velocity spectrum variation is nonlinear, the effective velocity variation is also nonlinear, based on Eq. (19).

The dashed line represents the effective velocity changes with the opening height. As the opening height increases, the pressure difference along the opening height will increase. Pelletret et al. [25] conducted several experiments for single-sided ventilation and found a nonlinear increase in the ventilation rate with the opening height. Our model (Eq. (13)) indicates that as the opening height increases, the pressure difference along the opening height will increase. Thus, this will result in a nonlinear increase of the ventilation rate or effective velocity, which agrees well with the findings from Pelletret et al.

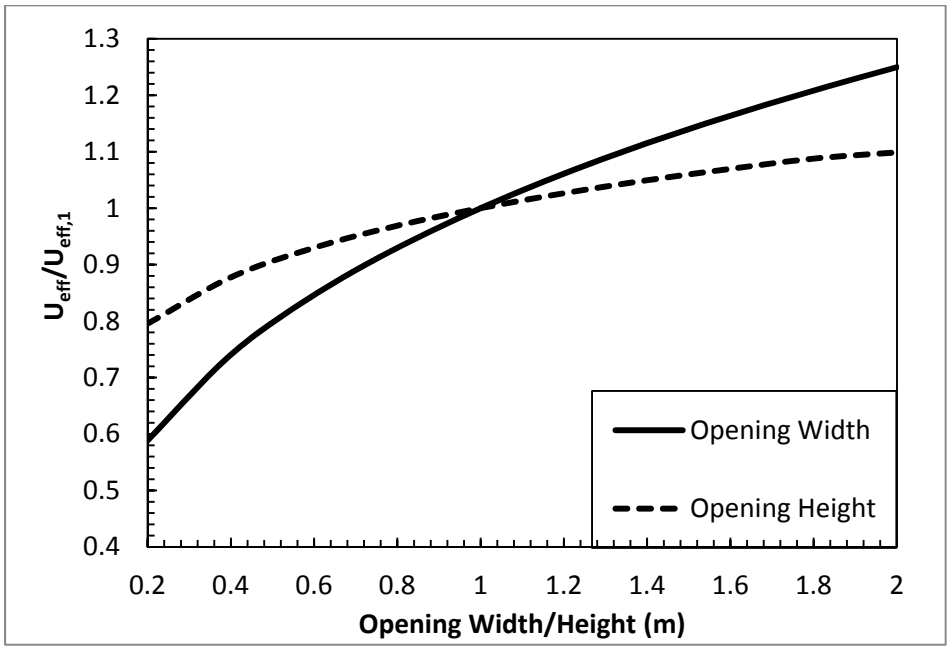

Figure 8 Normalized effective velocities for different opening widths and heights

The opening elevation to the ground can also influence the effective ventilation rate. As the elevation increases, the approaching wind velocity will also increase in the atmospheric boundary layer. Both an increase in wind velocity and elevation will have an influence on the ventilation rate. To differentiate the two factors, this investigation studied two cases: Elevation-1 and Elevation-2, as shown in Figure 9(a). Elevation-1 assumed an opening elevation change from 1 m to 2 m, but the wind velocity remained unchanged at 3.0 m/s. This is a case of changing wind profile as shown in the left figure of Figure 9(a). Elevation-2 changed the elevation but used the same wind profile so that the wind velocity at the opening would change. Figure 9(b) illustrates the impact of elevation on effective velocity for the two scenarios. The ventilation rate will decrease along with the elevation for both cases, due to the pressure decrease along the opening height. Scenario Elevation-2 has a higher ventilation rate than Scenario Elevation-1 because of the change of velocity in the opening.

Note that the above analysis is true for a building with only one opening. For single-sided ventilation with multiple openings, the result could be different since some openings will only have inflow and some will only have outflow. The governing force will be the wind pressure difference between each opening rather than the pressure difference along one opening height, as proposed in our models.

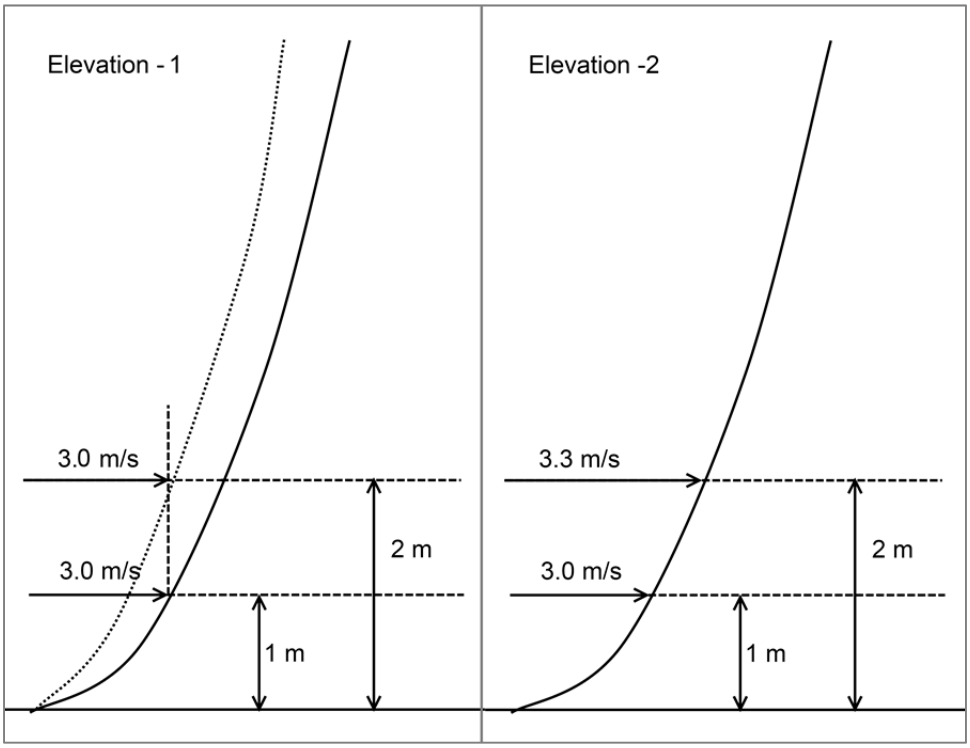

(a)

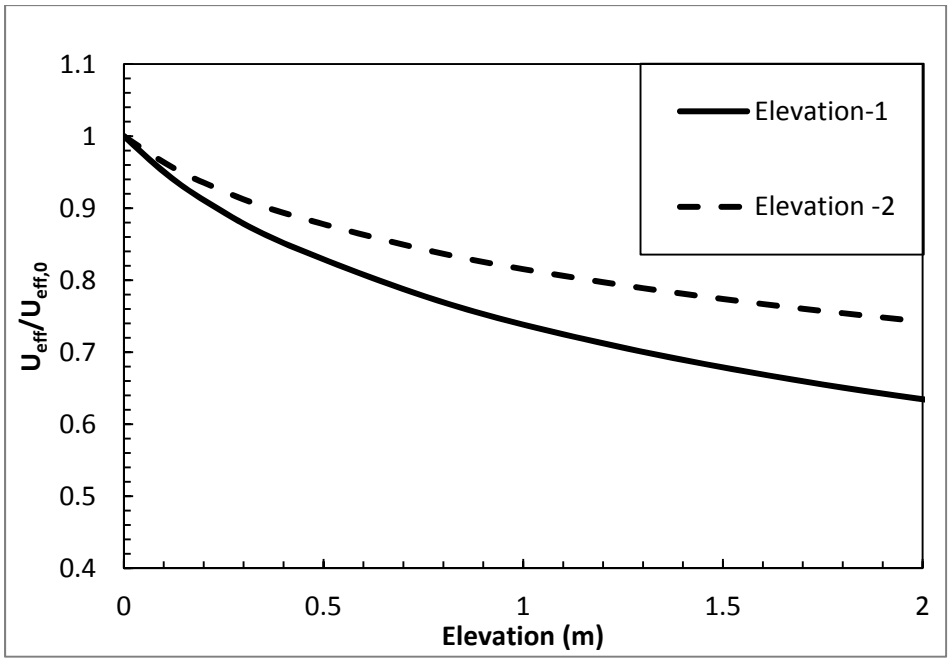

(b)

Figure 9 (a) The impact of opening elevation on ventilation rate (a) scenarios of elevation change and (b) normalized effective velocities for different elevations

5 Conclusion

This paper proposed new empirical models to predict a single-sided, wind-driven ventilation rate. The study led to the following conclusions:

1) Based on the pressure difference along an opening height, the empirical models can calculate the mean and the fluctuating ventilation rate through the opening. The fluctuating ventilation rate is a combination of pulsating flow and eddy penetration. This investigation used spectrum analysis to quantify the eddy penetration effect and has proved the eddy penetration to be a major factor when the wind is parallel to the opening.
2) CFD simulations of single-sided natural ventilation by LES were performed. The simulated results together with experimental data from the literature were used to validate the new empirical models. The differences between the empirical model predictions and CFD and/or the experimental data were less than 25%.
3) The profile of the normal velocity component at an opening can be predicted by our model, which also agrees with the CFD result.
4) This investigation also found that eddy penetration was zero when the wind incident angle was 0^o due to zero parallel velocity, and the penetration was low when the angle was around 70^o due to the low absolute pressure coefficient. The ventilation rate will

increase non-linearly with the opening size and will decrease as the opening elevation to the ground increases.

Acknowledgement

This research was supported by the U.S. Department of Energy through the Energy Efficient Buildings Hub.

6 References

[1] Energy information Agency, Annual Energy Review, 2011.

[2] ASHRAE Standard 55, Thermal environmental conditions for human occupancy, 2010.

[3] J. Finnegan, C. Pickering, and P. Burge, The sick building syndrome: prevalence studies, British Medical Journal 289 (1984) 1573-1575.

[4] P. Warren, Ventilation through openings on one wall only, in Energy conservation in Heating, Cooling and Ventilating, Dubrovnik, Yugoslavia, 1977.

[5] H. Phaff and W. De Gids, Ventilation rates and energy consumption due to open windows: a brief overview of research in the Netherlands, Air Infiltration Review 4 (1982) 4–5.

[6] T. Larsen and P. Heiselberg, Single-sided natural ventilation driven by wind pressure and temperature difference, Energy and Buildings 40 (2008) 1031–40.

[7] Marcello Caciolo, Pascal Stabat, and Dominique Marchio, Full scale experimental study of single-sided ventilation: analysis of stack and wind effects, Energy and Buildings 43 (2011) 1765-1773.

[8] F. Haghighat, J. Rao, and P. Fazio, The influence of turbulent wind on air change rates- a modeling approach, Building and Environment 26 (1991) 95-109.

[9] M. Straw, C. Baker, and A. Robertson, Experimental measurements and computations of the wind-induced ventilation of a cubic structure, Journal of Wind Engineering and Industrial Aerodynamics 88 (2000) 213-230.

[10] H. Malinowski, Wind effect on the air movement inside buildings, in Proceedings of the third international conference on wind on buildings and structures, Tokyo, 1971, 125-134.

[11] C. G. Lomas, Fundamentals of hot wire anemometry, Cambridge University Press, New York, 1986.

[12] Preben Buchhave and W. K. George Jr., The measurement of turbulence with the Laser-Doppler anemometer, Annual Review of Fluid Mechanics 11 (1979) 443-503.

[13] Yi Jiang and Qingyan Chen, Study of natural ventilation in buildings by large eddy simulation, Journal of Wind Engineering and Industrial Aerodynamics 89 (2001) 1155-1178.

[14] E. Dascalaki, M. Santamouris, and A. Argiriou, On the combination of air velocity and flow measurements in single sided natural ventilation configurations, Energy and Building 24 (1996) 155-165.

[15] G. Hellman, Uber die bewegung der luft in den untersten scichten der atmosphare, Meteorologische Zeitschrift 34 (1916) 273.

[16] M. Sherman and M. Modera, Comparison of measured and predicted infiltration using the LBL infiltration model, in Proceedings Measured Air Leakage of Buildings, Philadelphia, 1986, 325-347.

[17] F. Haghighat, Herik Brohus, and Jiwu Rao, Modeling air infiltration due to wind fluctuations – a review, Building and Environment 35 (2000) 377-385.

[18] Emil Simiu and Robert Scanlan, Wind Effects on Structures: An Introduction to Wind Engineering, Wiley-Interscience, New York,1986.

[19] Joseph Smagorinsky, General Circulation Experiments with the Primitive Equations, Monthly Weather Review 91 (1963) 99-164.

[20] ANSYS Inc., ANSYS FLUENT 12.0 Theory Guide, 2009.

[21] R. Kraichnan, Diffusion by a Random Velocity Field, Physics of Fluids 11 (1970) 21-31.

[22] R. Smirnov, S. Shi, and I. Celik, Random flow generation technique for large eddy simulations and particle-dynamics modeling, Journal of Fluids Engineering 123 (2001) 359-371,.

[23] G. Walton, Airflow and multiroom thermal analysis, ASHRAE Transactions 88 (1982) 78-91,.

[24] M. Swami and S. Chandra, Correlations for pressure distribution of buildings and calculation of natural-ventilation airflow, ASHRAE Transactions 94 (1988) 243-266.

[25] R. Pelletret, F. Allard, F. Haghighat, and J. Van der Maas, Modeling of large Openings, in Proceedings of 12th AIVC Conference, Ottawa, Canada, 1991.